



ELSEVIER

Cardiovascular Research 49 (2001) 751–761

---

---

*Cardiovascular  
Research*

---

---

www.elsevier.com/locate/cardiore  
www.elsevier.nl/locate/cardiore

## Intracellular calcium changes and tachycardia-induced contractile dysfunction in canine atrial myocytes

Hui Sun, Denis Chartier, Normand Leblanc, Stanley Nattel\*

*Research Center and Department of Medicine, Montreal Heart Institute, Departments of Medicine and Physiology, University of Montreal, and Department of Pharmacology, McGill University, 5000 Belanger Street East, Montreal, Quebec, Canada H3T 1C8*

Received 15 May 2000; accepted 13 November 2000

---

### Abstract

**Objectives:** Indirect evidence suggests a role for  $\text{Ca}^{2+}$ -overload in electrical and mechanical alterations caused by atrial tachycardia. The present study assessed the alterations in cellular  $[\text{Ca}^{2+}]_i$  and contractile function caused by rapid atrial cellular activation. **Methods:** Intracellular  $\text{Ca}^{2+}$  transients (CaT) and cell shortening (CS) were measured by microfluorometry (Indo-1 AM) and video edge-detection in isolated, field-stimulated canine atrial myocytes ( $37^\circ\text{C}$ ). **Results:** Abrupt increases in frequency (0.3–3 Hz) caused rapid increases in diastolic  $[\text{Ca}^{2+}]_i$  (DCa) that were maintained during rapid-pacing for up to 50 min. When short-term (3-min) rapid-pacing was imposed, CaT and CS increased initially upon returning to 0.3 Hz, but then declined rapidly to  $64 \pm 5$  and  $49 \pm 7\%$ , respectively, of pre-tachycardia values, returning to control after  $\sim 15$  min. Post-tachycardia CaT and CS reductions were prevented by decreasing  $[\text{Ca}^{2+}]_o$  during tachycardia to prevent  $\text{Ca}^{2+}$ -overload. CS reductions correlated with indices of  $\text{Ca}^{2+}$  loading during tachycardia. Restoration of CaT to normal during post-tachycardia contractile dysfunction (by increasing  $[\text{Ca}^{2+}]_o$ ) returned CS to normal, indicating that reduced  $\text{Ca}^{2+}$  release, not reduced myofilament  $\text{Ca}^{2+}$ -sensitivity, caused post-tachycardia contractile failure. Estimation of sarcoplasmic-reticulum  $\text{Ca}^{2+}$ -stores (caffeine-induced  $\text{Ca}^{2+}$ -release) confirmed tachycardia-induced  $\text{Ca}^{2+}$ -loading and suggested that reduced  $\text{Ca}^{2+}$ -stores decreased  $\text{Ca}^{2+}$ -release post-tachycardia. **Conclusions:** Atrial tachycardia increases cellular  $\text{Ca}^{2+}$ -loading, leading to post-tachycardia abnormalities in  $\text{Ca}^{2+}$ -handling that produce contractile dysfunction. These findings are the first direct evidence for the frequently-postulated role of  $\text{Ca}^{2+}$ -overload in tachycardia-induced abnormalities of atrial function. © 2001 Elsevier Science B.V. All rights reserved.

**Keywords:** Arrhythmia (mechanisms); Atrial function; Calcium (cellular); e-c coupling; Remodelling

---

### 1. Introduction

Rapid atrial activation, such as during atrial fibrillation (AF), changes atrial electrical and mechanical function [1,2]. Even brief periods of atrial tachycardia can abbreviate atrial refractoriness and cause contractile abnormalities [3–8]. Indirect evidence suggests that cellular  $\text{Ca}^{2+}$ -overload may play a role in the pathogenesis of electrical and mechanical dysfunction caused by both brief [4–8] and longer-lasting [9,10] atrial tachycardia; however, the effects of atrial tachycardia on intracellular  $\text{Ca}^{2+}$

concentration have not been directly measured. The present study was designed to record  $\text{Ca}^{2+}$  transients (CaT) and cell shortening (CS) in isolated canine atrial myocytes at slow rates and during tachycardia, in order to define any tachycardia-induced changes in intracellular  $[\text{Ca}^{2+}]_i$  fluctuations and to relate them to changes in CS.

### 2. Methods

The investigation conforms with the *Guide for the Care and Use of Laboratory Animals* published by the US

---

\*Corresponding author. Tel.: +1-514-376-3330; fax: +1-514-376-1355.

E-mail address: nattel@icm.umontreal.ca (S. Nattel).

**Time for primary review 25 days.**

National Institutes of Health (NIH Publication No. 85-23, revised 1996).

Adult mongrel dogs (20–30 kg) were anesthetized with morphine (2 mg/kg s.c.) and  $\alpha$ -chloralose (120 mg/kg i.v.) and mechanically ventilated. The heart was removed after intra-atrial injection of heparin (10 000 U), immersed in 2 mM  $\text{Ca}^{2+}$ -containing tyrode solution (TS) and the left atrium perfused via the circumflex artery with TS until clear of blood. The perfusate was then changed to nominally  $\text{Ca}^{2+}$ -free TS (20 min), after which 110 U/ml collagenase (Type 2, Worthington) and 0.1% BSA were added. Perfusion solutions were saturated with 100%  $\text{O}_2$  at 37°C. Cells were dispersed by gentle trituration in Tyrode's containing 10  $\mu\text{M}$  ( $\text{Ca}^{2+}$ ). The cells were kept at room temperature in TS with 100  $\mu\text{M}$  [ $\text{Ca}^{2+}$ ] and 0.1% BSA for use within 8 h. TS contained (mM) NaCl 136, KCl 5.4,  $\text{MgCl}_2$  1.0,  $\text{NaH}_2\text{PO}_4$  0.33, glucose 10, and HEPES 10; pH 7.4 (NaOH). The bath solution was TS with 0.4, 1.8 (standard solution), or 2.7 mM [ $\text{Ca}^{2+}$ ].

Myocytes were field-stimulated with 10-ms twice-threshold strength square-wave pulses. CS was measured with a video edge-detector connected to a charge-coupled device as previously described [11]. To record  $\text{Ca}^{2+}$  transients (CaT), myocytes were incubated with indo-1 AM (5- $\mu\text{M}$ ) for 5–7 min. Myocytes were then superfused at room temperature for at least 40 min to wash out extracellular indicator and to allow for deesterification. Background and cell autofluorescence were cancelled by zeroing the photomultiplier output in a cell without indo-1 loading. Ultra-violet light from a 100-W mercury arc lamp passing through a 340-nm interference filter ( $\pm 10$  nm bandwidth) was reflected by a dichroic mirror into a  $\times 40$  oil-immersion fluor objective for excitation of intracellular indo-1 (excitation beam  $\sim 15$   $\mu\text{m}$  diameter). Exposure of the cell to UV light (5–10 of every 30–60 s) was controlled by an electronic shutter (Optikon, model T132) to minimize photobleaching. Emitted light ( $< 550$  nm) was reflected into a spectral separator, passed through parallel filters at 400 and 500 nm ( $\pm 10$  nm), detected by matched photomultiplier-tubes (Hamamatsu R2560 HA) and electronically filtered at 60 Hz. The ratio of fluorescence signals ( $R_{400/500}$ ) was digitized (1 kHz) and used as the index of [ $\text{Ca}^{2+}$ ]<sub>i</sub> [12].

The bottom of the experimental chamber was treated with laminin to enhance cell adhesion. After cells had been loaded with indicator, the bath temperature was gradually increased to 35.5°C, and cells were stimulated at 0.3 Hz. When CaT and CS reached steady-state (usually in 5–10 min), stimulation frequency was abruptly increased to 3 Hz as specified below. In addition to standard bath-superfusion, a micro-tube connected to a temperature-controlled rapid solution-switching system was positioned to flow over the myocyte selected for study throughout each experiment in order to ensure constant conditions and rapid ( $< 500$  ms) perfusate changes.

Standard microelectrode techniques were used to record

intracellular action potentials from a multicellular right atrial preparation as previously described [13]. In brief, the right atrial free wall was removed and perfused at 20 ml/min via an atrial branch of the left circumflex coronary artery with Krebs–Henseleit solution (37°C) containing (mM) NaCl (120),  $\text{NaHCO}_3$  (25), KCl (4.2),  $\text{KH}_2\text{PO}_4$  (1.2),  $\text{MgSO}_4$  (1.2),  $\text{CaCl}_2$  (1.25) and glucose (11), equilibrated with 95%  $\text{O}_2$ /5%  $\text{CO}_2$ . A force transducer connected to the end of the preparation was used to record force generation. Floating KCl (3 M)-filled microelectrodes (tip resistances 15–30 M $\Omega$ ) were connected to an Axoclamp-2B amplifier via chlorided silver wire and a Ag–AgCl reference electrode was positioned in the bath.

CS was measured relative to diastolic cell length and the amplitude of CaT was measured as the difference between diastolic and maximal systolic fluorescence ratio ( $\Delta R_{400/500}$ ). The diastolic [ $\text{Ca}_i^{2+}$ ] (DCa) was measured as the  $R_{400/500}$  immediately before each activation. AP duration was calculated to 50% (APD 50) and 90% (APD 90) repolarization. The statistical significance of differences among groups was evaluated by one-way ANOVA followed by Duncan range tests. A two-tailed  $P < 0.05$  was considered significant. Group data are expressed as mean  $\pm$  S.E.M.

### 3. Results

#### 3.1. Effects of sustained tachycardia on CaT

Increasing the stimulation rate from 0.3 to 3 Hz caused a slight decrease in CaT and a gradual increase in DCa (Fig. 1A). Changes in DCa for nine myocytes observed during rapid stimulation for  $> 20$  min are shown in Fig. 1B. Of these cells, five lost 1:1 response at 14, 21, 23, 29 and 50 min of 3-Hz stimulation. In cells losing 1:1 responses, DCa remained elevated for over 2 min after returning to 0.3-Hz stimulation, whereas in the four other cells DCa returned to baseline level within 15 s. Fig. 1C shows mean DCa recorded in eight cells that followed 1:1 for at least 15 min at 3 Hz. DCa increased rapidly after the onset of rapid stimulation, approaching a plateau ( $\sim 15\%$  increase) by 2 min. In cells that lost 1:1 capture, a secondary phase of increasing DCa occurred prior to loss of capture (see Fig. 1B), suggesting that the latter was due to a loss of the ability to prevent excessive DCa increases. After confirming that 3-Hz stimulation causes sustained DCa increases, we evaluated the effects of transient (3-min) tachycardia on CaT and CS.

#### 3.2. Effects of transient tachycardia on CS and CaT

Fig. 2 shows representative continuous recordings of CS and CaT before, during and for 20 min after 3-Hz stimulation. Immediately after return to the basal frequency of 0.3 Hz, CS increased, and then declined rapidly

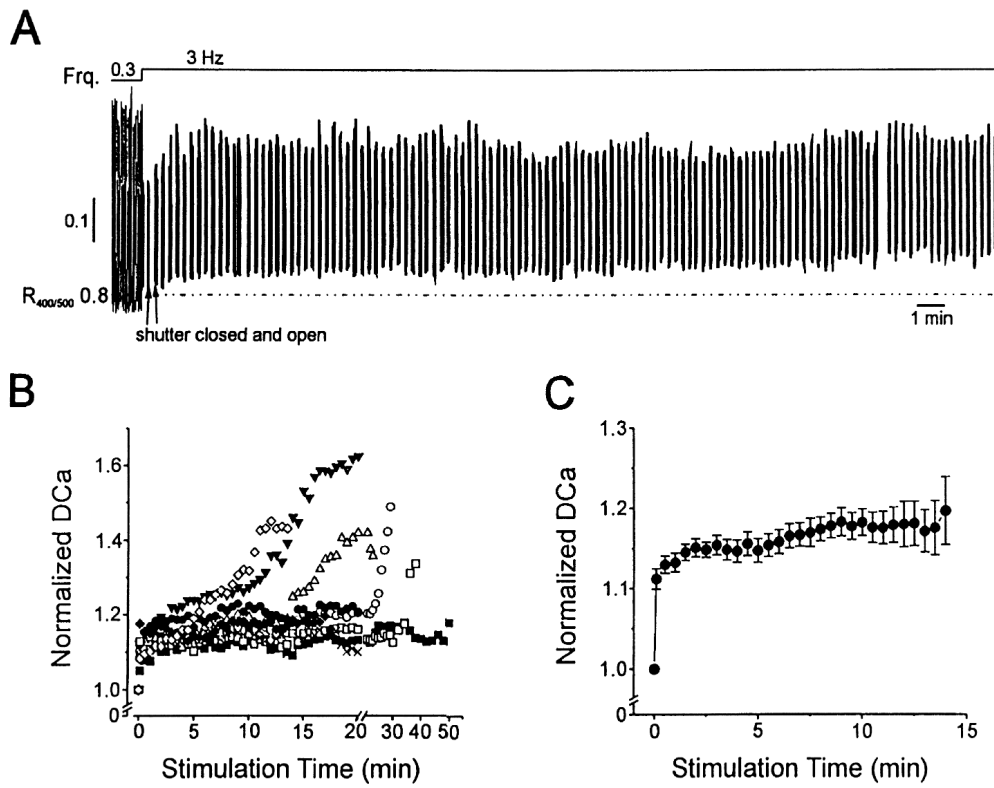


Fig. 1. (A) Representative recording of CaT when the stimulation frequency (*Frq*) was abruptly increased from 0.3 to 3 Hz. Spaces in the CaT recording correspond to electronic shutter closing to minimize cell exposure to UV light that can cause cell damage and Indo-1 photobleaching. Dashed line indicates resting  $R_{400/500}$  at 0.3 Hz. (B) DCa (each point mean over 10 s) normalized to pre-tachycardia values, during 3 Hz-stimulation for each of nine cells. (C) Mean normalized DCa in eight myocytes which maintained 1:1 stimulation at 3 Hz for  $\geq 15$  min.

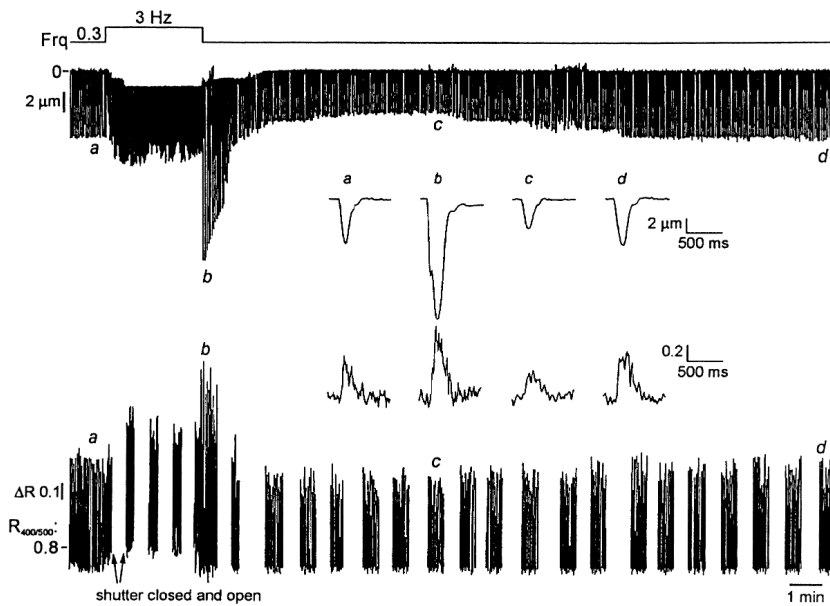


Fig. 2. Simultaneous recordings of CS (top) and CaT (bottom) in a cell submitted to 3 min of tachycardia. Stimulation frequency (*Frq*) is shown above recordings. Inset: recordings at times a, b, c, and d on expanded time scale.  $\Delta R$ :  $\Delta R_{400/500}$ .

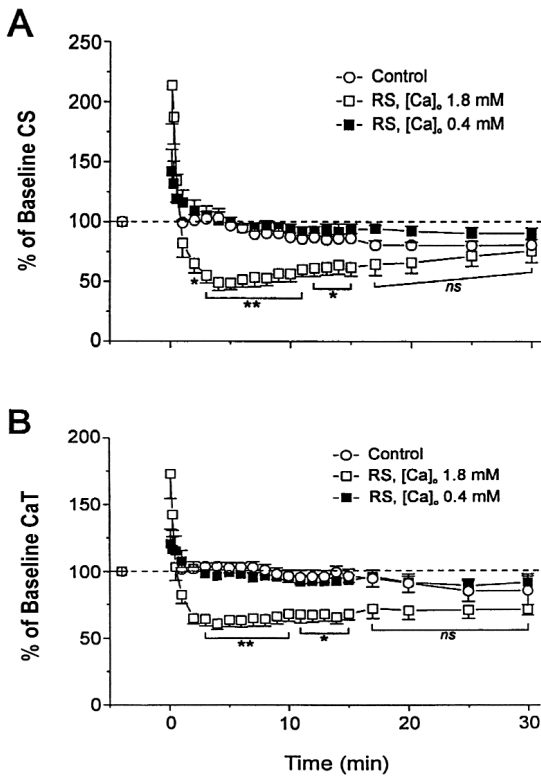


Fig. 3. Mean CS and CaT after cessation of 3-min rapid stimulation (3 Hz) in the presence of normal (1.8 mM,  $n=8$  cells) or low (0.4 mM,  $n=6$ )  $[Ca^{2+}]_o$ . A control group ( $n=5$ ) was followed for the same period with continuous 0.3 Hz stimulation. All values were normalized to pre-tachycardia baseline for each cell. \*  $P<0.05$ , \*\*  $P<0.001$  vs. control cells.

to about 60% of pre-tachycardia values by ~8 min. CS then recovered progressively, returning to control values after ~15 min. CaT showed a similar pattern of change to CS. DCa increased by 12% during tachycardia, but rapidly declined to control levels when the stimulation frequency was returned to 0.3 Hz.

Mean changes in CS and CaT after 3 min of rapid stimulation (RS) at 3 Hz in eight myocytes are shown in Fig. 3, along with values obtained from a control group of five cells stimulated at 0.3 Hz for the entire period. Transient tachycardia induced initial  $114\pm 32$  and  $73\pm 18\%$  increases in CS and CaT, respectively, for the second activation after returning to 0.3 Hz. CS and CaT then declined to  $49\pm 7$  and  $64\pm 5\%$  of pre-tachycardia values 4 min later. They then recovered, becoming non-significantly different from control within 15 min. DCa increased by  $9.8\pm 1.0\%$  during tachycardia ( $R_{400/500}$ :  $0.82\pm 0.06$  at 3 Hz vs.  $0.75\pm 0.06$  pre-tachycardia,  $P<0.001$ ), and declined to pre-stimulation levels within 10 s after returning to 0.3 Hz ( $0.74\pm 0.05$  vs.  $0.75\pm 0.06$ ).

### 3.3. Role of $Ca^{2+}$ loading in tachycardia-induced CS and CaT abnormalities

The data shown in Figs. 2 and 3 are consistent with a role for cellular  $Ca^{2+}$ -loading in CS and CaT abnormalities caused by transient tachycardia. We therefore examined the effects of decreasing  $Ca^{2+}$ -loading by decreasing  $[Ca^{2+}]_o$  to 0.4 mM during tachycardia. Fig. 4 shows recordings from a representative experiment. During tachycardia, the decreased  $[Ca^{2+}]_o$  resulted in reduced CS and CaT. Despite decreased  $Ca^{2+}$ -loading, a slight increase in DCa (by  $4.5\pm 0.8\%$ , resting  $R_{400/500}$ :  $0.82\pm 0.05$  vs.  $0.79\pm 0.05$

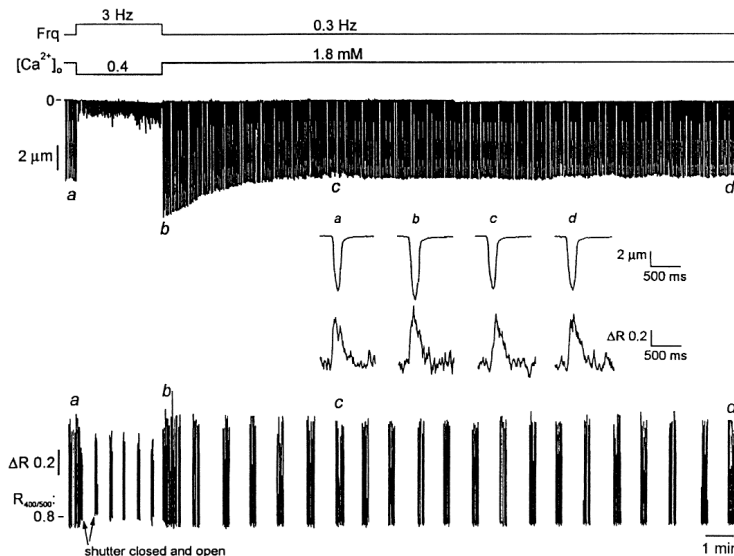


Fig. 4. Simultaneous recordings of CS (top) and CaT (bottom) in a cell exposed to reduced  $[Ca^{2+}]_o$  during tachycardia. Changes in stimulation frequency (Frq) and  $[Ca^{2+}]_o$  are indicated at top. Inset: CS and CaT recordings at times a, b, c, and d at an expanded time scale.  $\Delta R$ :  $\Delta R_{400/500}$ .

pre-tachycardia,  $P < 0.01$ ,  $n = 6$  cells) occurred. The return to 0.3 Hz and 1.8 mM  $[Ca^{2+}]_o$  was associated with an initial increase in CS and CaT; however, no subsequent reduction below baseline values occurred. Comparing insets b–d in Fig. 4 (recorded following tachycardia with  $[Ca^{2+}]_o$  reduced during tachycardia) with insets b–d in Fig. 2, it is apparent that decreased  $[Ca^{2+}]_o$  prevented tachycardia-induced CaT and contractile abnormalities. Mean data for post-tachycardia changes in CS and CaT following transient tachycardia in the presence of low  $[Ca^{2+}]_o$  are plotted in Fig. 3 ( $n = 6$  cells). Reducing  $Ca^{2+}$  influx during tachycardia attenuated the initial post-tachycardia increases in CS ( $114 \pm 32\%$  in control vs.  $42 \pm 19\%$  with reduced  $[Ca^{2+}]_o$ ,  $P < 0.05$ ) and CaT ( $73 \pm 18$  vs.  $21 \pm 11\%$ , respectively,  $P = 0.05$ ), and completely prevented the subsequent depression of CS and CaT.

If tachycardia-induced  $Ca^{2+}$ -loading is an important factor in post-tachycardia CS abnormalities, one would expect a positive relationship between tachycardia-induced CS decreases and DCa during tachycardia (reflecting the diastolic cytoplasmic  $[Ca^{2+}]$  rise) on one hand and the CaT (reflecting the amplitude of systolic  $Ca^{2+}$  release) on the other. Fig. 5 shows the relations between cytosolic  $Ca^{2+}$  during tachycardia and maximal post-tachycardia depression of CS in all 27 cells submitted to transient tachycardia. Highly-significant correlations were observed with both DCa (Fig. 5A,  $P < 0.001$ ) and CaT (Fig. 5B,  $P < 0.001$ ).

### 3.4. Role of post-tachycardia CaT decreases in CS abnormalities

To determine whether post-tachycardia  $Ca^{2+}$ -handling abnormalities can account for the associated CS abnormalities, we determined whether returning the CaT to normal during post-tachycardia contractile dysfunction can normalize CS. Fig. 6A shows recordings during a representative experiment. Initial increases in CS and CaT occurred immediately after 3 min of 3-Hz stimulation, followed by a typical decline to 54 and 68% of pre-stimulation values several minutes later. When CS and CaT were reduced, rapidly-switching  $[Ca^{2+}]_o$  from 1.8 to 2.7 mM increased both values. CS abnormalities returned when  $[Ca^{2+}]_o$  was returned to 1.8 mM and improved when  $[Ca^{2+}]_o$  was again increased. Mean results from eight myocytes are shown in Fig. 6B. Increasing  $[Ca^{2+}]_o$  during post-tachycardia contractile dysfunction raised the CaT to control values and restored CS, indicating that post-tachycardia contractile dysfunction is largely attributable to decreases in the systolic CaT.

### 3.5. Effects of transient tachycardia on sarcoplasmic reticulum (SR) $Ca^{2+}$ stores and the decay time course of the CaT

To explore further the mechanisms of tachycardia-re-

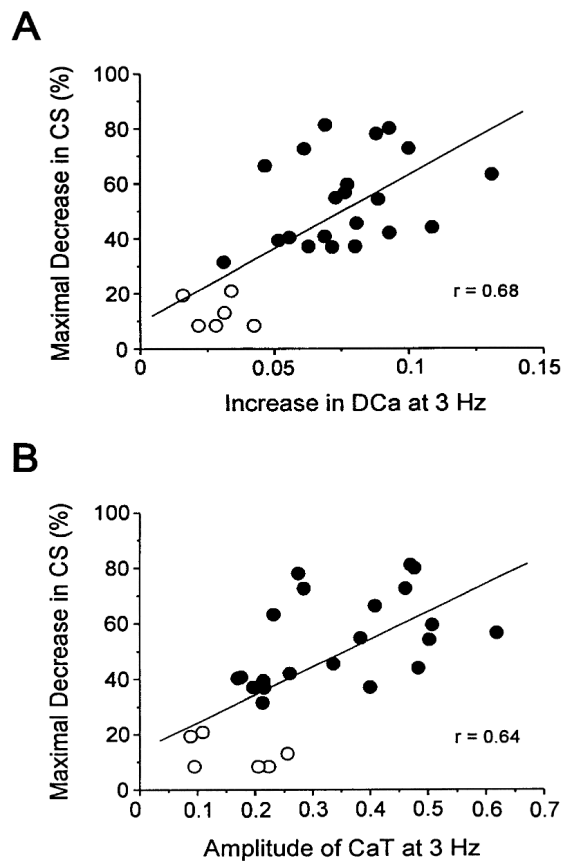


Fig. 5. Relations between maximal decreases in CS after short-term tachycardia and increases in DCa (A) and the amplitude of CaT (B) during rapid stimulation. Open symbols are results obtained with 0.4 mM  $[Ca^{2+}]_o$  and filled symbols are results at 1.8 mM  $[Ca^{2+}]_o$ . Lines are best-fit regressions.

lated  $Ca^{2+}$  handling abnormalities, we evaluated releasable SR  $Ca^{2+}$  stores with 10 mM caffeine (steady-state concentration achieved within 500 ms), which rapidly releases the  $Ca^{2+}$  in SR stores. Fig. 7A (top) shows recordings of the CaT response to caffeine before tachycardia (left) and at the time of hypocontractility, 5 min after the end of tachycardia (right). Post-tachycardia hypocontractility coincides with a decrease in caffeine-induced CaT, indicating decreased SR  $Ca^{2+}$  stores. Mean data for ten cells are shown in Fig. 7B (top), and indicate that tachycardia is followed by a significant decrease in SR  $Ca^{2+}$  stores. To exclude spontaneous time-dependent changes in SR  $Ca^{2+}$  stores, caffeine-induced  $Ca^{2+}$  release was studied at baseline and then after 15 min of stimulation at 0.3 Hz (middle panels of Fig. 7A,B). To evaluate SR  $Ca^{2+}$  stores during tachycardia, caffeine-induced  $Ca^{2+}$  release was measured immediately after 3-Hz stimulation for 3 min (bottom panels of Fig. 7A,B). The results confirm increased SR  $Ca^{2+}$  stores during tachycardia.

We also examined the kinetics of the CaT to evaluate

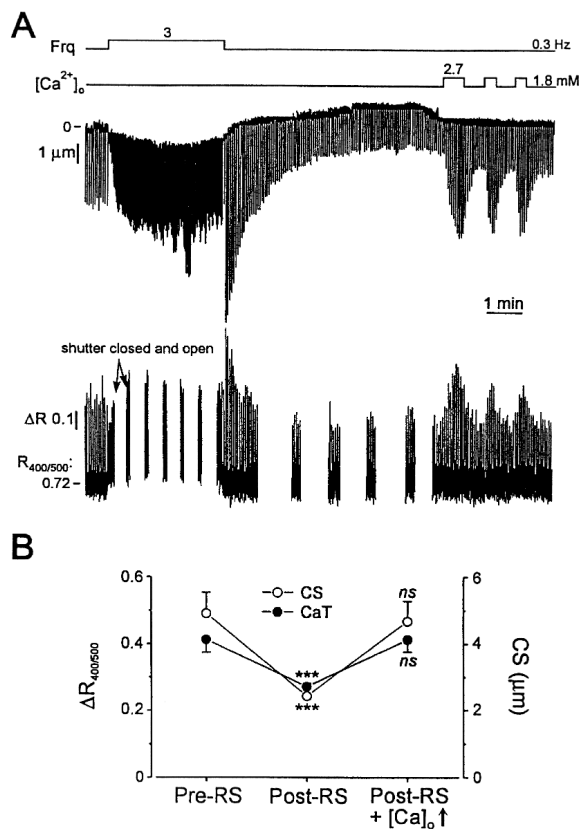


Fig. 6. (A) Representative recordings showing the effects of raising  $[Ca^{2+}]_o$  on tachycardia-induced depression of cellular contractile function. Changes in stimulation frequency ( $Frq$ ) and  $[Ca^{2+}]_o$  are indicated at top.  $\Delta R$ :  $\Delta R_{400/500}$ . (B) Mean  $\pm$  S.E.M. CS and CaT in eight cells subjected to increased  $[Ca^{2+}]_o$  during post-tachycardia contractile dysfunction. Values shown are pre-tachycardia baselines (Pre-RS), values during tachycardia-induced CS abnormalities (Post-RS), and values shortly thereafter when reduced CaT were increased by raising  $[Ca^{2+}]_o$  (Post-RS +  $[Ca^{2+}]_o \uparrow$ ). \*\*\*  $P < 0.001$ ; ns  $P > 0.05$  vs. pre-RS.

possible functional changes in  $Ca^{2+}$  handling. The rise time of the CaT was not significantly affected following tachycardia; however, CaT relaxation was slowed (Fig. 8). In 26 myocytes subjected to transient tachycardia, the time for 50% relaxation (based on a single-exponential curve fit to the decay time course) was increased by  $24 \pm 2\%$ , from  $207 \pm 5$  to  $257 \pm 6$  ms ( $P < 0.001$ ) 3 min after termination of tachycardia. No changes in CaT relaxation were seen in time-matched control myocytes stimulated continuously at 0.1 Hz or 3 min after 3-min stimulation at 3 Hz in the presence of low  $[Ca^{2+}]_o$ .

### 3.6. Effects of tachycardia on tension generation and APs in multicellular atrial preparations

Fig. 9A shows representative tension and AP recordings from an atrial preparation stimulated at 0.3 Hz and then

subjected to 3 min of tachycardia at 3 Hz. Following tachycardia, there is an initial period of hypercontractility, followed by transient hypocontractility and then gradual recovery. AP recordings show no major changes in morphology between baseline, hypercontractility post-tachycardia, hypocontractility and recovery conditions. In the multicellular preparations, it was possible to maintain 1:1 capture consistently at 5 Hz, which was not possible in single cells. Fig. 9B shows an experiment in which a multicellular preparation was subjected to 3-min tachycardia at 5 Hz after obtaining baseline recordings at 0.5 Hz. Upon returning to 0.5 Hz, periods of hyper- and hypocontractility were observed, followed by recovery. Mean data for experiments in multicellular preparations are shown in Fig. 10. Atrial tachycardia was followed by significant hyper- and then hypocontractility at both sets of frequencies studied. No significant changes in APD 90 were noted during hyper- or hypocontractility. For APD 50, no significant changes occurred at the time of hypocontractility for the 3-Hz protocol (Fig. 9A–c), but there was a significant reduction in the 5-Hz protocol. On the other hand, APD 50 was just as short for beat 3 post-tachycardia as for the time of hypocontractility in the 5-Hz protocol, despite normal tension generation for beat 3. Taken together, the data in Figs. 9 and 10 indicate that post-tachycardia changes in atrial contractility in multicellular atrial preparations are qualitatively similar to those in single cells, and that AP changes are unlikely to play a major role in these contractility changes.

## 4. Discussion

We found that atrial cellular tachycardia leads to  $Ca^{2+}$ -overload, and is followed by transient abnormalities in systolic  $Ca^{2+}$ -release and cell contraction. These abnormalities are correlated with indices of  $Ca^{2+}$ -loading during tachycardia, and can be prevented by reducing the  $Ca^{2+}$ -load by decreasing  $[Ca^{2+}]_o$  during rapid stimulation. Post-tachycardia contractile abnormalities are not due to persistent diastolic  $Ca^{2+}$  overload (Dca normalizes before CS abnormalities appear), and SR  $Ca^{2+}$  stores are reduced during post-tachycardia hypocontractility. Dysfunction of the  $Ca^{2+}$ -handling apparatus is likely central in contractile abnormalities, rather than a change in myofilament  $Ca^{2+}$  sensitivity, because restoration of the CaT during post-tachycardia contractile failure restores CS.

### 4.1. Cellular $Ca^{2+}$ loading as a result of atrial tachycardia

Leistad et al. [3] first suggested that short-lasting AF causes mechanical dysfunction by intracellular  $Ca^{2+}$  overload. Although several studies have pointed indirectly to  $Ca^{2+}$  overload in atrial tachycardia-induced remodeling [4,6–9], the present study is the first to show directly that

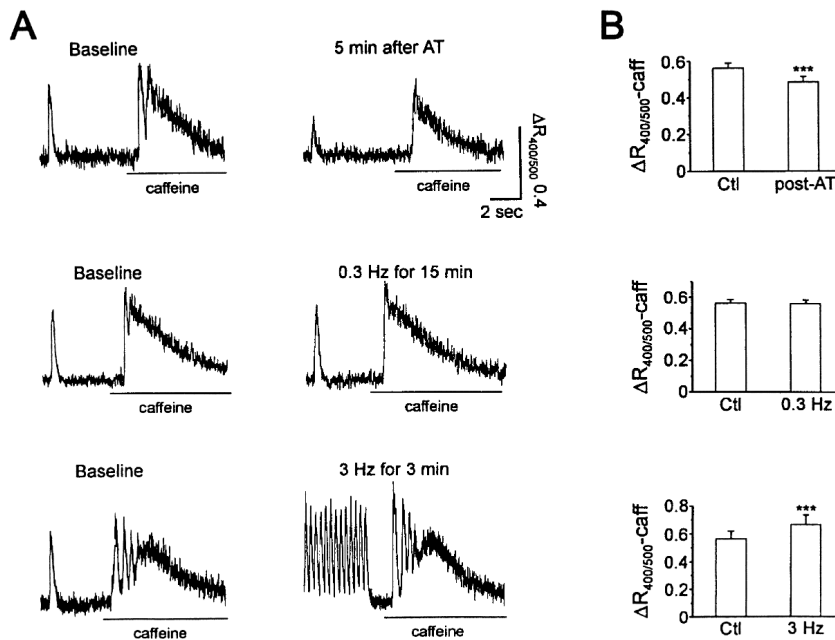


Fig. 7. (A) Representative recordings of caffeine-induced CaT. Caffeine (10 mM) was applied at the times indicated, under baseline conditions in each of three cells (left), and 3 min after returning to 0.3 Hz following transient tachycardia (AT, top right), after 15 min-stimulation at 0.3 Hz without tachycardia (middle, right) and immediately after termination of 3-min tachycardia (bottom, right). For each cell, after the baseline caffeine-induced CaT was recorded, the cell was allowed to rest for 1 min, and then stimulated at 0.5 Hz for 2 min to reload the SR, after which tachycardia was applied (top and bottom panels) or the cell was simply stimulated at 0.3 Hz (middle panel). (B) Mean  $\pm$  S.E.M. caffeine-induced CaT ( $\Delta R_{400/500}$ -caff) under baseline conditions (Ctl) and then following intervention illustrated to the left. \*\*\*  $P < 0.001$  vs. Ctl.

intracellular  $\text{Ca}^{2+}$  loading results from atrial tachycardia. Tachycardia increases  $\text{Ca}^{2+}$ -loading both directly by increasing the frequency of action potentials during which depolarization-induced  $I_{\text{Ca}}$  carries  $\text{Ca}^{2+}$  into the cell, and indirectly by increasing phase-0  $\text{Na}^+$  loading, with subsequent increased exchange of intracellular  $\text{Na}^+$  for extracellular  $\text{Ca}^{2+}$  via the  $\text{Na}^+/\text{Ca}^{2+}$ -exchanger [14]. Tachycardia also causes cellular  $\text{Ca}^{2+}$ -loading in ventricular tissue [14–19].

#### 4.2. $\text{Ca}^{2+}$ as a mediator of tachycardia-induced atrial contractile dysfunction

Impaired atrial mechanical function after reversion of acute AF was observed in a canine AF model over 30 years ago [20]. In dogs, AF for as brief as 5 min is followed by initial hypercontractility and then transient hypocontractility [3]. Contractile dysfunction is enhanced by the  $\text{Ca}^{2+}$ -agonist BayK8644 and prevented by the  $\text{Ca}^{2+}$ -antagonist verapamil [4]. In patients without structural heart disease, short-term AF (10–20 min) is followed by atrial hypocontractility, which can be prevented by verapamil [8]. Our study provides direct evidence for a mechanistic role of  $\text{Ca}^{2+}$ -loading, and suggests that contractile dysfunction is due to a persistent reduction in

systolic  $\text{Ca}^{2+}$  release caused by the effects of transient  $\text{Ca}^{2+}$ -overload on the  $\text{Ca}^{2+}$ -handling apparatus.

#### 4.3. Mechanisms underlying short-term tachycardia-induced atrial contractile dysfunction

Abnormal  $\text{Ca}^{2+}$ -handling and/or altered myofilament  $\text{Ca}^{2+}$ -responsiveness result in abnormalities in cellular contractility. The contractile dysfunction of stunned myocardium has been attributed to decreased myofilament  $\text{Ca}^{2+}$  responsiveness [21]. It has been proposed that  $\text{Ca}^{2+}$  overload during ischemia activates the  $\text{Ca}^{2+}$ -dependent protease, calpain I [22], which causes Troponin I proteolysis and thereby decreases myofilament  $\text{Ca}^{2+}$  sensitivity [23]. An involvement of abnormal  $\text{Ca}^{2+}$  handling in ischemia/reperfusion-induced myocardial contractile dysfunction has also been suggested [24]. Short-term exposure of ventricular myocytes to high  $[\text{Ca}^{2+}]_i$  decreases both systolic  $\text{Ca}^{2+}$  transients and myofilament  $\text{Ca}^{2+}$  sensitivity [25]. In the present study, we found no alteration of myofilament  $\text{Ca}^{2+}$  sensitivity: post-tachycardia CS abnormalities paralleled changes in  $\text{Ca}^{2+}$  transients and the post-tachycardia decrease in cell contraction was reversed by restoring the amplitude of  $\text{Ca}^{2+}$  transients to normal.

The precise mechanisms by which atrial tachycardia-

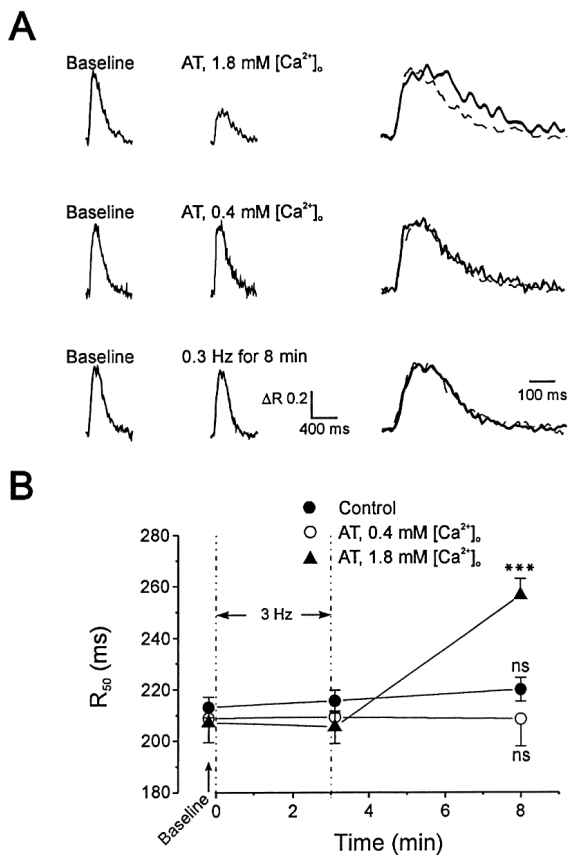


Fig. 8. Changes in the CaT decay time-course post-AT. (A) CaT under baseline conditions and 5 min after 3-min tachycardia (AT) in the presence of 1.8 (top) and 0.4 (middle) mM. Results at the bottom show corresponding data from parallel control experiments with cells stimulated at 0.3 Hz for 8 min. Recordings normalized to the pre-tachycardia amplitude are superimposed (baseline=dashed lines; AT recordings=solid lines) on a faster time base at the right. Each recording shown is the average of three consecutive recordings under each condition. The decay time course was fitted by single exponential functions and the time for 50% relaxation ( $R_{50}$ ) calculated. (B) Mean  $\pm$  S.E.M.  $R_{50}$  under baseline conditions, after 3 min of either AT or 0.3-Hz stimulation (control group), and 5 min after AT or after 8 min of 0.3-Hz stimulation (control group).  $n=7, 6$  and  $26$  cells for control, AT (0.4 mM [Ca<sup>2+</sup>]<sub>i</sub>) and AT (1.8 mM [Ca<sup>2+</sup>]<sub>i</sub>) groups, respectively. \*\*\* $P<0.001$  vs. baseline; ns=no significant difference vs. baseline.

induced Ca<sup>2+</sup> overload is followed by transient reductions in Ca<sup>2+</sup> release are unclear. Tachycardia increases SR Ca<sup>2+</sup> stores, producing increased CaT and contractility after tachycardia [14] which reverse rapidly as the SR discharges excess Ca<sup>2+</sup> at slower rates [26]. The subsequent transient reduction in the CaT may be due to decreased SR Ca<sup>2+</sup> stores and/or abnormalities in Ca<sup>2+</sup> release. The reduced caffeine-releasable Ca<sup>2+</sup> and slowed CaT relaxation we observed during post-tachycardia hypocontractility point to combined abnormalities in stores and the Ca<sup>2+</sup>-handling apparatus.

#### 4.4. Novel elements and potential significance

Post-AF atrial contractile dysfunction is important in thromboembolic complications after cardioversion of persistent AF [27–29]. Paroxysmal AF may also increase the risk of thromboembolic complications [30]. Repeated episodes of atrial contractile dysfunction after even relatively short episodes of AF may lead to sufficient stasis to promote thromboembolism, particularly if paroxysms are frequent. Understanding the mechanism of this phenomenon may be important in understanding the thromboembolic diathesis associated with paroxysmal AF and developing improved preventive strategies.

Our results may also be relevant to understanding mechanisms of atrial remodeling produced by longer-term tachycardia. It has been suggested that electrophysiological changes associated with atrial tachycardia-induced remodeling, such as down-regulation of L-type Ca<sup>2+</sup>-channel messenger RNA [31,32], protein [32,33] and current density [34–36], may be a response of the cell to prevent potentially-lethal Ca<sup>2+</sup> overload [2]. The present study, by showing that atrial cellular tachycardia does increase cellular Ca<sup>2+</sup> loading, contributes direct evidence for the hypothesized initial step of Ca<sup>2+</sup> loading. Our study also highlights differences between mechanisms of atrial contractile dysfunction caused by short-term versus long-term atrial tachycardia. Contractile dysfunction caused by long-term atrial tachycardia also accompanies CaT abnormalities, but normalization of the CaT fails to restore contractile function completely [11], unlike the effects of short-term tachycardia in the present study. Abnormalities in CaT caused by long-term tachycardia do not recover fully at slow rates, unlike the transient changes caused by short-term tachycardia. These observations are consistent with ultrastructural abnormalities caused by long-term atrial tachycardia [37,38], and with the notion that the changes caused by short-term tachycardia are due to functional rapidly-reversible adaptations, whereas longer-term tachycardia leads to changes in gene expression and cell composition that reverse more slowly, if at all [2,39].

In our study, Ca<sup>2+</sup>-overload led to secondary abnormalities in Ca<sup>2+</sup>-release that reduced CaT amplitude and consequently decreased CS. The degree of Ca<sup>2+</sup>-loading during tachycardia correlated with post-tachycardia contractile dysfunction, providing a potential rationale for the effectiveness of previously-used strategies (such as verapamil administration) to reduce tachycardia-related Ca<sup>2+</sup> loading in preventing post-tachycardia contractile dysfunction [4,8]. Calpain II, a predominant cytoplasmic form of Ca<sup>2+</sup>-dependent protease in cardiac muscle, selectively digests the SR Ca<sup>2+</sup> release channel, increasing its open probability and impairing inactivation [40]. It has been suggested that calpain II activation in Ca<sup>2+</sup>-overload states would result in defective SR Ca<sup>2+</sup>-uptake, as in acute myocardial ischemia [40]. Defective SR Ca<sup>2+</sup> uptake could account for all the post-tachycardia Ca<sup>2+</sup>-handling abnor-

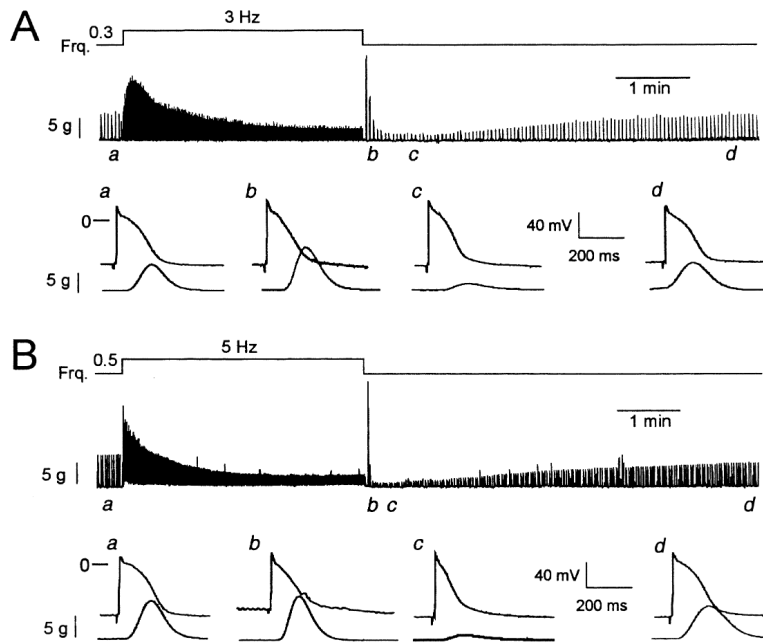


Fig. 9. Effects of atrial tachycardia on tension generation and APs in representative multicellular atrial preparations. (A) Continuous tension recording (top) and individual APs and tension recordings (bottom) obtained at times indicated before, immediately after, at the time of maximum hypocontractility and after recovery in a preparation subjected to AT at 3 Hz (Frq.=frequency). (B) Corresponding data for a preparation subjected to AT at 5 Hz.

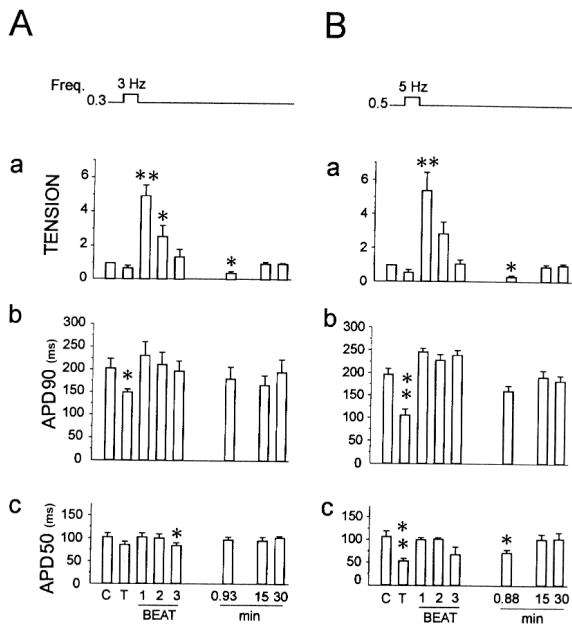


Fig. 10. Mean  $\pm$  S.E.M. normalized tension (a), APD 90 (b) and APD 50 (c) from preparations subjected to AT at 3 Hz (A,  $n=5$ ) and 5 Hz (B,  $n=6$ ). Results are shown under baseline conditions (C), at the end of 3 min of tachycardia (T), for beats 1, 2 and 3 following tachycardia, at maximum post-tachycardia hypocontractility (mean time=0.93 min for 3 Hz, 0.88 min at 5 Hz) and 15 and 30 min post-tachycardia.  $**P<0.05$ , 0.01 vs. control, respectively.

malities we observed: decreased SR  $Ca^{2+}$  stores, a reduced CaT and slowed relaxation of the CaT signal.

#### 4.5. Advantages and limitations of the model

The present study was performed in isolated atrial myocytes, in order to visualize intracellular  $Ca^{2+}$  simultaneously with cell contraction. The isolated cell system avoids limitations imposed in vivo by endogenous automaticity, altered autonomic tone, neurohumoral changes and hemodynamic alterations. One potential disadvantage is that cell isolation may damage cells, introducing potential artifacts. Severe damage is unlikely in our cells, since they were able to maintain  $Ca^{2+}$  homeostasis, generate normal  $Ca^{2+}$  release patterns and maintain mechanical activity for significant periods of time. In addition, cellular contractile dysfunction paralleled changes in our multicellular preparations and previous observations in vivo [3,4].

It would have been interesting to know absolute values of  $[Ca^{2+}]_i$ , rather than simply expressing  $[Ca^{2+}]_i$  in terms of the  $R_{400/500}$  ratio. It is possible to calibrate the indicator for  $[Ca^{2+}]_i$  in aqueous solutions, but this may be misleading since the properties of  $Ca^{2+}$ -sensitive dyes in the cytoplasm are different from those in aqueous solution. In vivo  $Ca^{2+}$  indicator calibration also involves a number of uncertainties [12].

## 5. Conclusions

Rapid activation of atrial myocytes causes cellular  $\text{Ca}^{2+}$ -overload, which results in transiently impaired  $\text{Ca}^{2+}$ -release and cellular contractile function after cessation of a brief period of tachycardia. Impaired  $\text{Ca}^{2+}$ -release is the major mechanism of depressed cellular contractile function following short-term atrial tachycardia.

## Acknowledgements

The authors thank Chantal St-Cyr for technical assistance and Diane Campeau and France Thériault for help with the manuscript. This work was supported by the Medical Research Council of Canada and the Quebec Heart Foundation.

## References

- [1] Wijffels MC, Kirchhof CJ, Dorland R, Allesie MA. Atrial fibrillation begets atrial fibrillation: a study in awake chronically instrumented goats. *Circulation* 1995;92:1954–1968.
- [2] Nattel S. Atrial electrophysiological remodeling caused by rapid atrial activation: underlying mechanisms and clinical relevance to atrial fibrillation. *Cardiovasc Res* 1999;42:298–308.
- [3] Leistad E, Christensen G, Ilebek A. Atrial contractile performance after fibrillation. *Am J Physiol* 1993;264:H104–H109.
- [4] Leistad E, Aksnes G, Verburg E, Christensen G. Atrial contractile dysfunction after short-term atrial fibrillation is reduced by verapamil but increased by BAY K8644. *Circulation* 1996;93:1747–1754.
- [5] Daoud EG, Bogun F, Goyal R et al. Effect of atrial fibrillation on atrial refractoriness in humans. *Circulation* 1996;94:1600–1606.
- [6] Daoud EG, Knight BP, Weiss R et al. Effect of verapamil and procainamide on atrial fibrillation-induced electrical remodeling in humans. *Circulation* 1997;96:1542–1550.
- [7] Yu WC, Chen SA, Lee SH et al. Tachycardia-induced changes of atrial refractory period in humans: rate dependency and effects of antiarrhythmic drugs. *Circulation* 1998;97:2331–2337.
- [8] Daoud EG, Marcovitz P, Knight BP et al. Short-term effect of atrial fibrillation on atrial contractile function in humans. *Circulation* 1999;99:3024–3027.
- [9] Goette A, Honeycutt C, Langberg JJ. Electrical remodeling in atrial fibrillation: time course and mechanisms. *Circulation* 1996;94:2968–2974.
- [10] Tieleman RG, De Langen CD, Van Gelder IC et al. Verapamil reduces tachycardia-induced electrical remodeling of the atria. *Circulation* 1997;95:1945–1953.
- [11] Sun H, Gaspo R, Leblanc N, Nattel S. Cellular mechanisms of atrial contractile dysfunction caused by sustained atrial tachycardia. *Circulation* 1998;98:719–727.
- [12] Bassani JWM, Bassani RA, Bers DM. Calibration of indo-1 and resting intracellular  $[\text{Ca}]_i$  in intact rabbit cardiac myocytes. *Biophys J* 1995;68:1453–1460.
- [13] Lu Y, Yue L, Wang Z, Nattel S. Effects of the diuretic agent indapamide on  $\text{Na}^+$ , transient outward, and delayed rectifier currents in canine atrial myocytes. *Circ Res* 1998;83:158–166.
- [14] Boyett MR, Frampton JE, Harrison SM et al. The role of intracellular calcium, sodium and pH in rate-dependent changes of cardiac contractile force. In: Noble MIM, Seed WA, editors, *The interval-force relationship of the heart: Bowditch revisited*. New York: Cambridge University Press, 1992, pp. 111–172.
- [15] Langer GA. Calcium exchange in dog ventricular muscle: relation to frequency of contraction and maintenance of contractility. *Circ Res* 1965;17:78–89.
- [16] Lado MG, Sheu SS, Fozzard HA. Changes in intracellular  $\text{Ca}^{2+}$  activity with stimulation in sheep cardiac Purkinje strands. *Am J Physiol* 1982;243:H133–H137.
- [17] Lee HC, Clusin WT. Cytosolic calcium staircase in cultured myocardial cells. *Circ Res* 1987;61:934–939.
- [18] Thandroyen FT, Morris AC, Hagler HK et al. Intracellular calcium transients and arrhythmia in isolated heart cells. *Circ Res* 1991;69:810–819.
- [19] Koretsune Y, Marban E. Cell calcium in the pathophysiology of ventricular fibrillation and in the pathogenesis of postarrhythmic contractile dysfunction. *Circulation* 1989;80:369–379.
- [20] Macieira-Coelho E, Alves MG, Almiro H, Coelho E. Atrial activity following conversion of experimental atrial fibrillation by direct current shock. *Acta Cardiol* 1968;23:439–453.
- [21] Bolli R, Marban E. Molecular and cellular mechanisms of myocardial stunning. *Physiol Rev* 1999;79:609–634.
- [22] Gao WD, Liu Y, Mellgren R, Marban E. Intrinsic myofilament alterations underlying the decreased contractility of stunned myocardium. *Circ Res* 1996;78:455–465.
- [23] Gao WD, Atar D, Liu Y, Perez NG, Murphy AM, Marban E. Role of troponin I proteolysis in the pathogenesis of stunned myocardium. *Circ Res* 1997;80:393–399.
- [24] Meissner A, Morgan J. Contractile dysfunction and abnormal  $\text{Ca}^{2+}$  modulation during postischemic reperfusion in rat heart. *Am J Physiol* 1995;268:H100–H111.
- [25] Holt E, Christensen G. Transient  $\text{Ca}^{2+}$  overload alters  $\text{Ca}^{2+}$  handling in rat cardiomyocytes: effects on shortening and relaxation. *Am J Physiol* 1997;273:H537–H582.
- [26] Bers D. Control of cardiac contraction by SR Ca release and sarcolemmal Ca fluxes. In: Bers D, editor, *Excitation-contraction coupling and cardiac contractile force*. Dordrecht: Kluwer, 1991, pp. 149–170.
- [27] Grimm RA, Stewart WJ, Maloney JD et al. Impact of electrical cardioversion for atrial fibrillation on left atrial appendage function and spontaneous echo contrast: characterization by simultaneous transesophageal echocardiography. *J Am Coll Cardiol* 1993;22:1359–1366.
- [28] Fatkin D, Kuchar DL, Thorburn CW, Feneley MP. Transesophageal echocardiography before and during direct current cardioversion of atrial fibrillation: evidence for ‘atrial stunning’ as a mechanism of thromboembolic complications. *J Am Coll Cardiol* 1994;23:307–316.
- [29] Black IW, Fatkin D, Sagar KB et al. Exclusion of atrial thrombus by transesophageal echocardiography does not preclude embolism after cardioversion of atrial fibrillation: a multicenter study. *Circulation* 1994;89:2509–2513.
- [30] The Stroke Prevention in Atrial Fibrillation Investigators. Predictors of thromboembolism in atrial fibrillation: I. Clinical features of patients at risk. *Ann Intern Med* 1992;116:1–5.
- [31] Yue L, Melnyk P, Gaspo R, Wang Z, Nattel S. Molecular mechanisms underlying ionic remodeling in a dog model of atrial fibrillation. *Circ Res* 1999;84:776–784.
- [32] Brundel BJM, Van Gelder IC, Henning RH et al. Gene expression of proteins influencing the calcium homeostasis in patients with persistent and paroxysmal atrial fibrillation. *Cardiovasc Res* 1999;42:443–454.
- [33] Gaspo R, Sun H, Fareh S et al. Dihydropyridine and beta adrenergic receptor binding in dogs with tachycardia-induced atrial fibrillation. *Cardiovasc Res* 1999;42:434–442.
- [34] Yue L, Feng J, Gaspo R, Li GR, Wang Z, Nattel S. Ionic remodeling underlying action potential changes in a canine model of atrial fibrillation. *Circ Res* 1997;81:512–525.

- [35] Van Wagoner DR, Pond AL, Lamorgese M, Rossie SS, McCarthy PM, Nerbonne JM. Atrial L-type  $\text{Ca}^{2+}$  currents and human atrial fibrillation. *Circ Res* 1999;85:428–436.
- [36] Bosch RF, Zeng X, Grammer JB, Popovic K, Mewis C, Kühlkamp V. Ionic mechanisms of electrical remodeling in human atrial fibrillation. *Cardiovasc Res* 1999;44:121–131.
- [37] Morillo CA, Klein GJ, Jones DL, Guiraudon CM. Chronic rapid atrial pacing. Structural, functional, and electrophysiological characteristics of a new model of sustained atrial fibrillation. *Circulation* 1995;91:1588–1595.
- [38] Ausma J, Wijffels M, Thone F, Wouters L, Allesie M, Borgers M. Structural changes of atrial myocardium due to sustained atrial fibrillation in the goat. *Circulation* 1997;96:3157–3163.
- [39] Allesie MA. Atrial electrophysiologic remodeling: another vicious circle? *J Cardiovasc Electrophysiol* 1998;9:1378–1393.
- [40] Rardon DP, Cefali DC, Mitchell RD, Seller SM, Hathaway DR, Jones LR. Digestion of Cardiac and skeletal muscle junctional sarcoplasmic reticulum vesicles with calpain II. Effects on the  $\text{Ca}^{2+}$  release channel. *Circ Res* 1990;67:84–96.